Automatic Evaluation Algorithm for Intersection Hole Cylindrical Feature in on Machine Measurement Operation

Andri Pratama[1], Yogi Muldani Hendrawan[1][a], Andini Eka Rahmani[1], Nizar Miftah Ilyasa[1], Herman Budi Harja[1], Muhammad Udin Harun Al Rasyid[2][b] and Idris Winarno[2]

[1]Department of Manufacturing Engineering Technology, Politeknik Manufaktur Bandung, Dago, Bandung, Indonesia
[2]Department of Informatics and Computer Engineering, Politeknik Elektronika Negeri Surabaya, Sukolilo, Surabaya, Indonesia

Keywords: CAIP, OMM, Feature Recognition, Intersection Cylindrical Feature.

Abstract: This paper discusses an algorithm that can automatically evaluate the intersection hole feature. It takes input data probe, data reference, data measurement, and ISO 2768 tolerance database to run algorithms on software which is programmed by the python language. The test model that has the counterbore and countersink features is tested on an algorithm whose results will then be presented in the form of a standard QC sheet. The results of OMM measurements will be compared with manual standard measurements to determine the performance of the algorithm.

1 INTRODUCTION

The manufacturing industry is constantly trying to meet market demands and satisfy customers. To realize this, technological developments in the manufacturing process should be more effective and efficient. One of them, automation of manufacturing processes in production process which is not produce added value directly. This process is a process that requires time, resources, and capacity but does not increase product value directly, such as the process of setting the machine, inspection, and delivery (Abdul and Musazali, 2020). The inspection process has the opportunity to make more efficient in manufacturing process because the inspection process time is depend on the number of functional dimensions in a product.

By On-Machine Measurement (OMM), inspection process can be done in CNC machine. So the workpiece not need to be removed from CNC machine (Chen et al., 2016; Ding et al., 2020; Huang et al., 2018; Liu et al., 2015; Mutilba et al., 2017). The automation inspection process can be developed by implemented Computer Aided Inspection Planning (CAIP) on the On-Machine Measurement (OMM) system (Chung, 1999). It is an integrated process that involves designing, machining, and inspecting the manufacturing process to measure products directly at the machine. While CAIP is a product modelling system that can describe the need for intelligent geometry and dimension measurements. CAIP is divided into four stages, face detection, feature reconstruction, inspection planning, and inspection code generated (Hendrawan et al, 2014). Thus, CAIP and OMM are a combination that allows the OMM method to automate and integrate the inspection process. In conducting OMM inspections, which requires feature properties information from the extracted feature reconstruction phase (Hendrawan et al, 2021) as input inspection code generated.

After the measurement which is using the OMM method has been successfully generated (Hendrawan et al., 2021), the next step is to compare the data from the initial two-stage output on the CAIP and the results of the OMM measurement. This activity is called post CAIP which will give a GO or NO GO decision on the condition of the hole that has been made. This paper focuses on intersection hole cylindrical feature such as the counterbore and countersink features which are often found in manufactured products or fasteners application, especially.

[a] https://orcid.org/0000-0003-4774-4966

[b] https://orcid.org/0000-0002-4473-2364

2 HOLE PROPERTIES EVALUATION

This algorithm focuses on the double hole feature including counterbore and countersink. The dimension parameters of the size and position of the two features that will be evaluated by this algorithm. Therefore, information about the feature properties of the hole is needed.

2.1 Counterbore Properties

Detailed counterbore feature properties information will be shown in the image below.
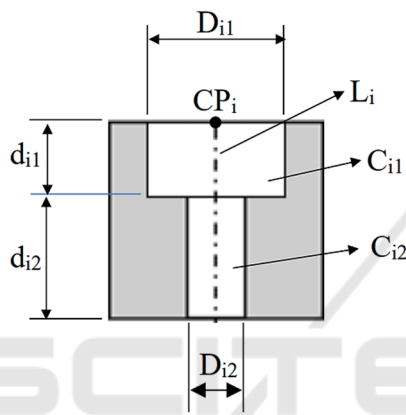
Figure 1: Countersink properties. Source: (Hendrawan et al, 2021).

Basically, counterbore consists of two single hole features that are on the same axis, namely the blind hole and the through hole, each of which has diameter and depth information as shown in Fig. 1. Di1, Di2, Cpi, Li, di1, di2, Ci1, and Ci2 are top circular diameter, bottom circular diameter, centre point, line axis, top depth, bottom depth, top cylindrica, and bottom cylindrical in i^{th} feature, respectively.

To evaluate this counterbore feature requires the condition that $D_{i1}>D_{i2}$ and di1 as the depth evaluated from the inbus bolt head that becomes the counterbore hole pair. CPi will only be represented by CPx and CPy coordinates. The counterbore feature information that needed for evaluation is $D_{i1}, D_{i2}, d_{i1},$ CPx and CPy.

2.2 Countersink Properties

Detailed feature properties information of countersink will be shown in the image below.
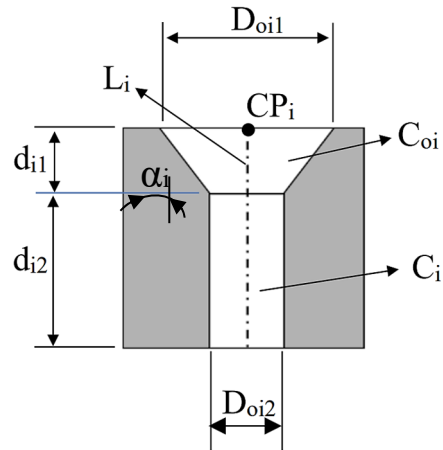
Figure 2: Counterbore properties. Source: (Hendrawan et al, 2021).

Countersink consists of a tapered hole and through hole that are on the same axis. The built tapered feature consists of the upper diameter, bottom diameter, and depth are represented by D_{oi1}, D_{oi2}, and d_{i1}, respectively with the provisions of $D_{oi1}> D_{oi2}$ which can form an αi angle with the following formula.

$$\alpha_i = tan^{-1}(\frac{Doi1-Doi2}{2di1}) \quad (1)$$

$$di1 = \frac{Doi1-Doi2}{2tan\alpha i} \quad (2)$$

Where $\alpha i = 45º$ is set according to the standard. CPi is represented as CPx dan CPy. The countersink feature information that needed for evaluation is $D_{oi2},$ $d_{i1}, CPx,$ and CPy.

3 MEASUREMENT METHODS

To evaluate based on the feature properties that have been defined, a measurement cycle method is needed, namely the diameter measurement cycle and the depth measurement cycle.

3.1 Hole Measurement Cycle

In taking measurements by On Machine Measurement on the hole cylindrical feature, a hole measurement cycle is required which is stated as follows.

```
;R07=DIAMETER
;R19=WORK_OFFSET_G54_G59

L9800
R07=40.R19=2.
L9023
M30
```
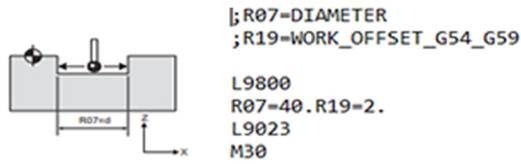
Figure 3: Measure hole illustration. Source: (Renishaw, 2014).

After the hole measurement cycle is executed by a machine that has installed a probe interface and PRIMO™ system from RENISHAW, measurement results in the form of diameter and centre points of the hole (X and Y) can be produced.

3.2 Depth Measurement Cycle

In addition to the hole measurement cycle, a depth measurement cycle is needed to complete the measurements on the hole cylindrical feature. The depth measurement cycle is expressed as follows.


```
;R19=WORK_OFFSET_G54_G59

L9800
R26=-10.R19=1.
L9023
M30
```
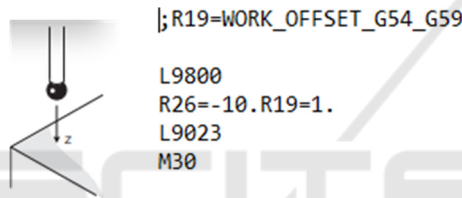
Figure 4: Measure depth illustration Source: (Renishaw, 2014).

Results in the form of depth in the hole can be produced After the depth measurement cycle is executed by the machine that has installed the probe interface and primo™ system from RENISHAW.

4 AUTOMATIC HOLE EVALUATION

To complement the previously proposed hole evaluation module which is only for single-hole features, a hole evaluation module was added to evaluate the double hole feature which certainly enhances the four stages already implemented.

4.1 Inspection Code Generator

With the definition of the cycle to be used as well as the planning of the probe path that has been generated. So an inspection code generator was formed in accordance with existing standards. Therefore, the measurement touching points

information is needed. To define touching points on the counterbore, Eq. (3) is used as follows:

$$tp_{probe} = cp_{i_z} - Øprobe \qquad (3)$$

a. Touching points for measuring diameter pilot hole counterbore:

$$tp_{probe} = cp_{i_z} - (1.3 \times d_{i_1}) \qquad (4)$$

b. Touching points for measuring counterbore depth:

In defining touching points for measuring depth. It takes a shift in the centre point (X) expressed as follows.

- If the *center1_cbn* value is positive

$$move\_center = (cp_{i_x}) - ((r\,cp_{i_x}) - 0.05) \qquad (5)$$

- If the *center1_cbn* value is negative

$$move\_center = (cp_{i_x}) - ((r\,cp_{i_x}) + 0.05) \qquad (6)$$

After the central point shift value (X) is generated, the next step is to execute the cycle for depth measurement.

Meanwhile, the measurement touching points is defined to measure countersink. The presence of differences due to the profile in this type of hole is oblique. Thus, it can be concluded that the touching point for depth measurement cannot be carried out and replaced to make the countersink Ø measurement which is stated as follows.

$$hypotenouse = \frac{(d_{i_1})}{\cos(\alpha_i)} \qquad (7)$$

$$tp\_probe = cp_{i_z} - 3 \qquad (8)$$

$$new\_hypo = \frac{-(tp\_probe) \times hypotenouse}{d_{i_1}} \qquad (9)$$

$$deviation\_new = ((tp\_probe)) + (new\_hypo) \qquad (10)$$

$$tp_{probe_{new}} = (deviation\_new) + (tp\_probe) \qquad (11)$$

After the measurement for the Ø countersink is carried out, the next step is to measure the Ø pilot hole on the countersink by below equation.

$$tp_{probe} = cp_{i_z} - (1.3 \times d_{i_1}) \qquad (12)$$

4.2 Hole Evaluation Module

By calculating the difference value between the feature properties data which is created by the previously algorithm to evaluate the single hole feature, and feature properties information from the double hole which is added with measurement result data that becomes increased depending on their respective features. For this reason, probe path data,

feature properties data, measurement data that has been added, and ISO 2768 tolerance data are needed. Due to the limitations of the measurement method, the depth of the countersink feature can be calculated using Eq. (1). The difference in evaluation for each parameter entering the tolerance area will be given a GO decision while the difference outside the tolerance area will be given a NO GO decision.

5 EXPERIMENT

To prove that the proposed algorithm can be applied, the algorithm was tested at the Hyundai WIA F510M Vertical Machining Centre with a SIEMENS 828D controller as shown in Fig. 5 and a measurement tool the 3D probe RENISHAW PRIMO to conduct experiments.

Figure 5: VMC Hundyai WIA f510M.

The machines used have travel axes of X 1060 mm, Y 635 mm, Z 635 mm, and table dimensions of 1200 mm x 500 mm, respectively. The 3D diameter size of the Renishaw PRIMO probe selected is 6mm to take measurements at the inspection stage of the code generator. The measurement results will be directly tested on proposed software that has been embedded with an evaluation module programmed using the Python language.
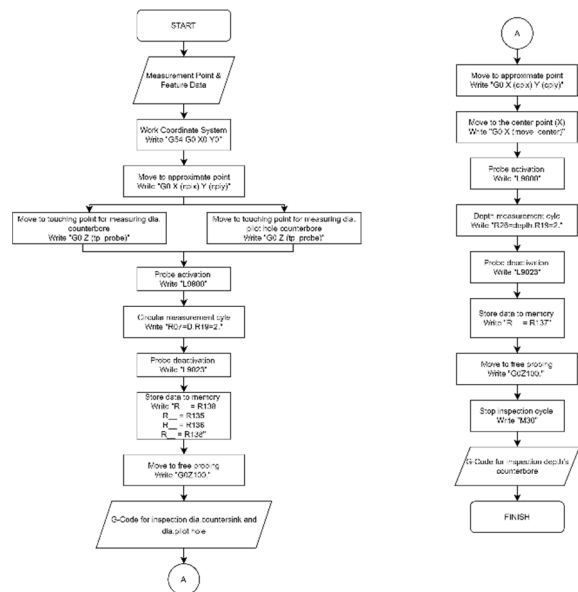
Figure 6: Inspection code algorithm.
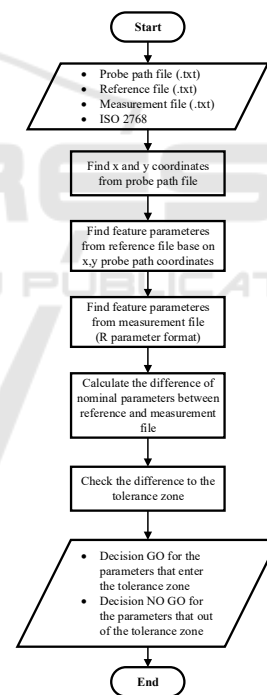
Figure 7: Hole evaluation algorithm.

5.1 Experimental Scenario

The G-Code generated at the inspection stage of the generator code will be tested on a workpiece that features an M12 counterbore with details of the upper diameter of 20 mm, a lower diameter of 13.5 mm, and a depth of 12.8 mm as well as an M10 countersink hole with details of a lower diameter of 11 mm, a

depth of 5.7 mm, and an angle of 45 degrees as shown in Fig.8.
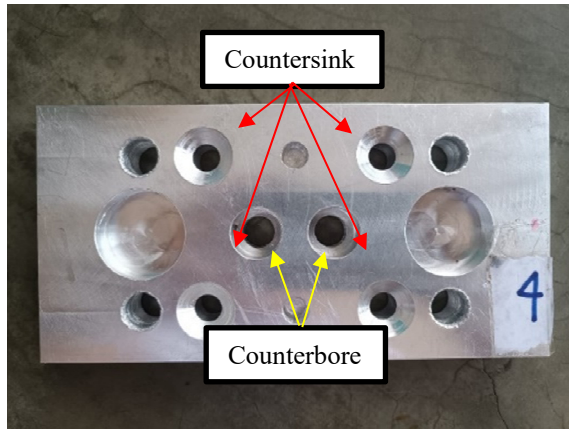
Figure 8: Product specimen.

The error results from the measurements will be compared to the medium tolerance range listed in ISO 2768 automatically. The results of the evaluation will be listed in a standard QC sheet format. To validate the measurement results directly on the machine, standard manual measurements were carried out using a vernier calliper with a precision of 0.02 mm because the evaluation was still based on moderate tolerances.

5.2 Experimental Result

The evaluation results are listed as shown with the full information listed in the table.

Figure 9: Holes Evaluator interface.

It was found that counterbores 1 and 2 with actual sizes and positions respectively are the upper diameters of 20.035 mm and 19.985 mm, the lower

diameters of 13.339 mm and 13.350 mm, the depths of 12.811 mm and 12.821 mm, the X coordinates of 14.996 mm and -14.966 mm, and finally the Y coordinates of 0.048 mm and 0.010 mm. For other features, countersinks 1, 2, 3, and 4 respectively obtained bottom diameters of 11,046 mm, 10.961 mm, 11.045 mm, and 11.032 mm, depths of 5,662 mm, 5,702 mm, 5,668 mm, and 5,672 mm, X coordinates 34.994 mm, 34.968 mm, -34.991 mm, and -34.994 mm, and finally coordinates Y -30.000 mm, 29.995 mm, 30.008 mm, and -29.986 mm. The differences from the counterbore features are the upper diameters of 0.035 and -0.014, the lower diameters of -0.160 mm and -0.149 mm, the depths of 0.011 mm and 0.021 mm., the X coordinates -0.003 mm and 0.033 mm, and the Y coordinates 0.0487 mm and 0.010 mm. The differences for the countersink feature were obtained successively, namely the lower diameters of 0.046 mm, -0.038 mm, 0.045 mm, and 0.032 mm, depths -0.038 mm, 0.002 mm, -0.032 mm, and -0.028 mm, X coordinates -0.005 mm, -0.031 mm, 0.008 mm, and 0.005 mm, as well as coordinates Y -0.0009 mm, -0.004 mm, 0.008 mm, and 0.013 mm. All parameters evaluated for both the counterbore and countersink features are categorized GO because they fall within the tolerance range.

The second experiment is to validate the measurement results on the machine by a vernier calliper to evaluate all parameters evaluated in on-machine measurement. The difference results for the counterbore feature were obtained respectively, namely the upper diameters of 0.04 mm and -0.016 mm, the lower diameters of -0.156 mm and -0.16 mm, depths of -0.012 mm and -0.004 mm, X coordinates -0.002 mm and 0.032 mm, and coordinates of Y -0.014 mm and -0.004 mm. For the countersink feature obtained successively, namely the lower diameters of 0.008 mm, -0.044 mm, 0 mm, and 0.004 mm, depths of 0.05 mm, 0.06 mm, 0.03 mm, and 0.02 mm, X coordinates 0 mm, -0.026 mm, 0.02 mm, and 0.018, and finally coordinate Y -0.06 mm, -0.014 mm, -0.044 mm, and -0.004 mm. All parameters evaluated by using the calliper are categorized GO because they fall within the tolerance range as shown in table 1 and 2.

When viewed from the experiments of the hole evaluation algorithm automatically and measuring it manually, both show the same decision results, namely GO for all the parameters evaluated. This means that the proposed algorithm has proven to be correct in providing decisions by comparing the results of measurements manually using calipers.

6 CONCLUSIONS

The proposed algorithm already evaluates the counterbore and countersink features. The proposed algorithm is developed and implemented in software programmed using the Python language. Experiments are needed to test the performance of the algorithm. The software created requires probe path data, feature properties data as a reference, measurement data on the machine, and ISO 2768 tolerance database as input data. The parameters evaluated are the upper diameter, lower diameter, depth, x coordinate, and y coordinate of the counterbore feature as well as the lower diameter, depth, X coordinate, and Y coordinate of the countersink feature. The evaluation results are displayed in a standard QC sheet format. Based on the experiments that have been carried out, the algorithm can already work properly.

No	Feature	Dim		Std	Tol	Result	Error	Status
1	CB1	Du 20		20.0	0.2	20.0354	0.0354	GO
		Dl 13.5		13.5	0.2	13.3395	-0.1605	GO
		De 12.8		12.8	0.2	12.8112	0.0112	GO
		CP	X	15.0	0.2	14.9967	-0.033	GO
			Y	0.0	0.1	0.0106	0.04875	GO
2	CB2	Du 20		20.0	0.2	19.9853	-0.0147	GO
		Dl 13.5		13.5	0.2	13.3503	-0.1497	GO
		De 12.8		12.8	0.2	12.8212	0.0212	GO
		CP	X	-15.0	0.2	-14.96605	0.03395	GO
			Y	0.0	0.1	0.0106	0.0106	GO
3	CS1	Dl 11		11.0	0.2	11.046	0.046	GO
		De 5.7		5.7	0.1	5.662	-0.038	GO
		CP	X	35.0	0.3	34.9943	-0.0057	GO
			Y	-30.0	0.2	-30.00095	-0.00095	GO
4	CS2	Dl 11		11.0	0.2	10.9614	-0.0386	GO
		De 5.7		5.7	0.1	5.702	0.002	GO
		CP	X	35.0	0.3	34.9681	0.0319	GO
			Y	30.0	0.2	29.9955	-0.0045	GO
5	CS3	Dl 11		11.0	0.2	11.0453	0.0453	GO
		De 5.7		5.7	0.1	5.668	-0.032	GO
		CP	X	-35.0	0.3	-34.99135	0.00865	GO
			Y	30.0	0.2	30.008	0.008	GO
6	CS4	Dl 11		11.0	0.2	11.0323	0.0323	GO
		De 5.7		5.7	0.1	5.672	0.0319	GO
		CP	X	-35.0	0.3	-34.99465	0.00535	GO
			Y	-30.0	0.2	-29.9867	0.0133	GO

Figure 10: Automatic hole evaluation result (mm).

ACKNOWLEDGEMENTS

No	Feature	Dim		Std	Tol	Result	Error	Status
1	CB1	Du 20		20.0	0.2	20.004	0.004	GO
		Dl 13.5		13.5	0.2	13.344	-0.156	GO
		De 12.8		12.8	0.2	12.788	0.012	GO
		CP	X	15.0	0.2	14.998	-0.002	GO
			Y	0.0	0.1	-0,014	-0.014	GO
2	CB2	Du 20		20.0	0.2	19.984	-0.016	GO
		Dl 13.5		13.5	0.2	13.34	-0.16	GO
		De 12.8		12.8	0.2	12.796	-0.004	GO
		CP	X	-15.0	0.2	-14.968	0.032	GO
			Y	0.0	0.1	-0.004	-0.004	GO
3	CS1	Dl 11		11.0	0.2	11.008	0.008	GO
		De 5.7		5.7	0.1	5.75	0.05	GO
		CP	X	35.0	0.3	35.0	0.0	GO
			Y	-30.0	0.2	-30.06	-0.06	GO
4	CS2	Dl 11		11.0	0.2	10.956	-0.044	GO
		De 5.7		5.7	0.1	5.76	0.06	GO
		CP	X	35.0	0.3	34.974	-0.026	GO
			Y	30.0	0.2	29.986	-0.014	GO
5	CS3	Dl 11		11.0	0.2	11.0	0.0	GO
		De 5.7		5.7	0.1	5.73	0.03	GO
		CP	X	-35.0	0.3	-34.98	0.02	GO
			Y	30.0	0.2	29.956	-0.044	GO
6	CS4	Dl 11		11.0	0.2	11.004	0.004	GO
		De 5.7		5.7	0.1	5.72	0.02	GO
		CP	X	-35.0	0.3	-34.982	0.018	GO
			Y	-30.0	0.2	-29.998	0.002	GO

Figure 11: Manual hole evaluation result.

REFERENCES

Abdul Rasib, A.H., Musazali, M. (2020). Undestanding of Non-Value Added Overtime in Manufacturing Operations. In IOP Conference Series: Material Science and Engineering. doi: 10.1088/1757-899X/994/1/012004

Chung, S.C. (1999). CAD/CAM Integration of on-the-machine measuring and inspection system for free formed surfaces. Proceedings of American Society for Precision Engineering, vol.20, pp 267-270.

Hendrawan, Y.M., Yuwana, M.Y., and Raharno, S. (2014). Development of computer aided inspection planning (CAIP) application in on machine measurement operation (OMM) operations for box primitive features: Generating inspection codes. In Applied Mechanics and Materials, vol 660, pp.889-893.

Chen, Y. L., Cai, Y., Shimizu, Y., Ito, S., Gao, W., & Ju, B. F. (2016). On-machine measurement of microtool wear and cutting edge chipping by using a diamond edge artifact. *Precision Engineering*, *43*, 462–467. https://doi.org/10.1016/j.precisioneng.2015.09.011

Ding, D., Zhao, Z., Zhang, X., Fu, Y., & Xu, J. (2020). Evaluation and compensation of laser-based on-machine measurement for inclined and curved profiles. *Measurement*, *151*, 107236. https://doi.org/10.1016/j.measurement.2019.107236

Huang, N., Yin, C., Liang, L., Hu, J., & Wu, S. (2018). Error compensation for machining of large thin-walled part with sculptured surface based on on-machine measurement. *International Journal of Advanced Manufacturing Technology*, *96*(9–12), 4345–4352. https://doi.org/10.1007/s00170-018-1897-x

Liu, H. B., Wang, Y. Q., Jia, Z. Y., & Guo, D. M. (2015). Integration strategy of on-machine measurement (OMM) and numerical control (NC) machining for the large thin-walled parts with surface correlative constraint. *International Journal of Advanced Manufacturing Technology*, *80*(9–12), 1721–1731. https://doi.org/10.1007/s00170-015-7046-x

Hendrawan, Y.M., Muttaqin, R., Pratama, A., Budi Harja, H., Udin, M., al Rasyid, H., & Winarno, I. (2021). *Intersection Cylindrical Feature Recognition Algorithm for Counterbore and Countersink Geometry Application*.

Hendrawan, Y.M., Pratama, A., Budi Harja, H., Udin, M., al Rasyid, H., & Winarno, I. (2021). *Inspection Code Generator for Hole Cylindrical Feature Evaluation in On-Machine Measurement Process for Computer Aided Inspection Planning*.

Mutilba, U., Gomez-Acedo, E., Kortaberria, G., Olarra, A., & Yagüe-Fabra, J. A. (2017). Traceability of on-machine tool measurement: A review. In *Sensors (Switzerland)* (Vol. 17, Issue 7). MDPI AG. https://doi.org/10.3390/s17071605

Renishaw. (2014). "Easyprobe cycle for machining center," *Programming Guide*, no, H-2000-6294-00-B